https://doi.org/10.20965/jrm.2018.p0971

Paper:

Low-Altitude and High-Speed Terrain Tracking Method for Lightweight AUVs

Toshihiro Maki*, Yukiyasu Noguchi*, Yoshinori Kuranaga*, Kotohiro Masuda*, Takashi Sakamaki*, Marc Humblet, and Yasuo Furushima*****

*Institute of Industrial Science, The University of Tokyo
4-6-1 Komaba, Meguro-ku, Tokyo 153-8505, Japan
E-mail: maki@iis.u-tokyo.ac.jp
**Department of Earth and Planetary Sciences, Nagoya University
Furo-cho, Chikusa-ku, Nagoya 464-8601, Japan
E-mail: humblet.marc@f.mbox.nagoya-u.ac.jp
***Japan Agency for Marine-Earth Science and Technology
2-15 Natsushima, Yokosuka, Kanagawa 237-0061, Japan
E-mail: furus@jamstec.go.jp

[Received April 14, 2018; accepted October 29, 2018]

This paper proposes a new method for cruising-type autonomous underwater vehicles (AUVs) to track rough seafloors at low altitudes while also maintaining a high surge velocity. Low altitudes are required for visual observation of the seafloor. The operation of AUVs at low altitudes and high surge velocities permits rapid seafloor imaging over a wide area. This method works without high-grade sensors, such as inertial navigation systems (INS), Doppler velocity logs (DVL), or multi-beam sonars, and it can be implemented in lightweight AUVs. The seafloor position is estimated based on a reflection intensity map defined on a vertical plane, using measurements from scanning sonar and basic sensors of depth, attitude, and surge velocity. Then, based on the potential method, a reference pitch angle is generated that allows the AUV to follow the seafloor at a constant altitude. This method was implemented in the AUV HATTORI, and a series of sea experiments were carried out to evaluate its performance. HATTORI (Highly Agile Terrain Tracker for Ocean Research and Investigation) is a lightweight and low-cost testbed designed for rapid and efficient imaging of rugged seafloors, such as those containing coral reefs. The vehicle succeeded in following a rocky terrain at an altitude of approximately 2 m with a surge velocity of approximately 0.8 m/s. This paper also presents the results of sea trials conducted at Ishigaki Island in 2017, where the vehicle succeeded in surveying the irregular, coral-covered seafloor.

Keywords: autonomous underwater vehicle (AUV), seafloor observation, scanning sonar, path planning, obstacle avoidance

1. Introduction

Photographic survey of the seafloor is considered an effective method to obtain detailed information about the color and shape of objects down to sub-millimeter sizes, and it can be used for a wide range of applications in various fields, such as biology, fishery, resource exploration, archeology, search and rescue, and maintenance of artificial structures. Recent advancements in underwater robotics have led to the development of autonomous underwater vehicles (AUVs) which are suitable for wide-area seafloor photo-mosaicing [1–6].

Owing to strong light attenuation, an AUV has to be close to the seafloor to perform photographic surveys. The ideal shooting distance depends on a number of factors including water quality, characteristics of floating particles, ambient light, performance of the imaging apparatus, required image quality, required coverage, and available lighting. Based on our experience with hydrothermal vent fields, the typical shooting distance varies between 1.0 and 3.0 m [2, 7]. Torpedo-shaped cruising-type AUVs can be used for this task when the terrain is relatively flat. For example, the AUV HUGIN has been used for visual inspection of pipelines [8]. On the other hand, so-called hovering-type AUVs are suitable for rough terrains, such as coral reefs, hydrothermal vent fields, and ship wrecks [9, 10]. They can stop and vertically ascend if they detect a steep wall in front of them, whereas cruising-type AUVs are at high risk of collision with large obstacles. However, hovering-type AUVs are much slower than cruising-type AUVs, with typical surge velocities between 0.1 to 0.5 m/s, due to their complicated shape and relatively large profile. Therefore, imaging rough terrains is currently a time-consuming process compared with other survey types, such as bathymetry or water quality surveys.

This paper proposes a method for a cruising-type AUV to follow rugged terrains at a low altitude that is suitable for photographic surveys, while maintaining a surge velocity much higher than that of the typical hovering-type AUVs. The authors hope that the new method will enable rapid imaging of rugged seafloors. Another purpose of the proposed method is to reduce the cost of seafloor imaging. Most of current AUVs suitable for seafloor imaging are heavy, requiring a crane-equipped vessel for their operation; moreover, expensive sensors such as high-grade inertial navigation systems (INS), Doppler velocity logs (DVL), and multi-beam sonars are required to keep the vehicle at a low altitude over rough terrains. As the proposed method involves only standard sensors, it can be implemented in low-cost, lightweight AUVs. This publication is an extended version of a conference paper on the same topic [11] and provides more detailed information on the new terrain tracking method. Results of experiments in and around the Sekisei Lagoon, a large lagoon enclosed by a coral reef west of Ishigaki Island, demonstrate the feasibility of the proposed method and reliability of our testbed AUV HATTORI.

In this paper we first describe in detail the proposed method, then we introduce our testbed vehicle HATTORI, and finally, we present the results of the sea trials.

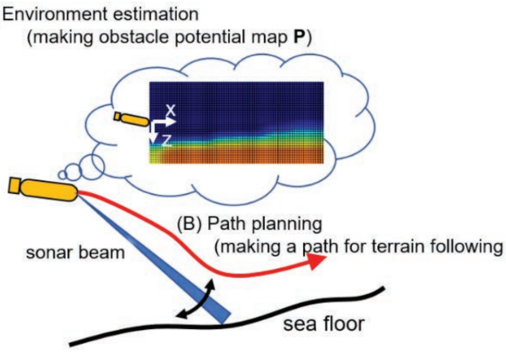

Fig. 1. Concept of the proposed method.

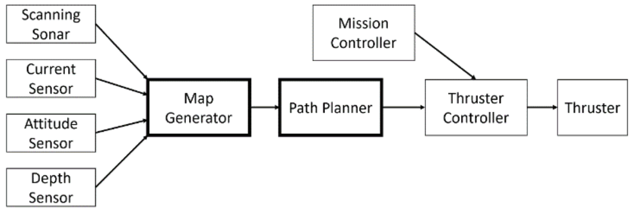

Fig. 2. Block diagram of the proposed method.

2. Terrain Tracking Method

2.1. Related Work

Due to its large surge velocity and limited maneuverability, a cruising-type AUV must recognize the forward environment and plan desirable paths much more quickly than a hovering-type AUV. McPhail et al. proposed a scanning sonar based method [12, 13]. In their method, an AUV tries to fly over any obstacles initially and, if this proves to be impossible, the AUV retreats while decreasing its depth. The imminence of collision is evaluated based on the distance and height of an obstacle ahead. A scanning sonar is mounted on the vehicle's nose and it is operated in the vertical plane. An auxiliary parameter called "pseudo altitude" is calculated from the sonar measurements. The lower values of both the "pseudo altitude" and an altitude measured by a separate altitude sensor are used to calculate the deviation from a reference altitude. Schillai et al. estimated the risk of collision of an AUV over known terrains to get a better understanding of the factors determining the collision risk [14]. Noguchi et al. proposed an application of machine learning technology for AUV navigation in which a reference pitch angle is generated by a reinforcement learning agent based on the scanning sonar readings [15].

The potential method is a well-known technique for the path planning of mobile robots. Applying the method to underwater vehicles has been also proposed [16, 17]. However, most previous works depend on using a multi-beam sonar. Although a multi-beam sonar can detect obstacles in a wide range of directions at once, it is difficult to mount on a small, low-cost vehicle. Furthermore, to the knowledge of the authors, most previous works use the potential method for horizontal path planning or obstacle avoidance and not for vertical terrain tracking underwater.

2.2. Concept

The purpose of the proposed terrain tracking method is to track rough terrains, such as coral reefs, at low altitudes suitable for visual survey, for example, 2 m, while maintaining a relatively high surge velocity, typically several knots. The other purpose is to achieve the above goal without relying on high-grade sensors, such as an INS, DVL, or multi-beam sonar. It is assumed that the heading angle and surge velocity of the vehicle are maintained constant, while the roll angle is always set to zero. This method controls only the pitch angle to track the terrain.

The concept and block diagram of the method are shown in **Figs. 1** and **2**, respectively. A scanning sonar is used to detect the seafloor ahead of the vehicle, and then a reference path is generated. The method consists of two steps: environment estimation (map generator) and path planning (path planner).

The advantage of the proposed method is that the raw measurements of the scanning sonar, i.e., the intensities of the reflected sound wave, are directly used to estimate the seafloor location, without any thresholding. This makes it possible to detect weak signals from the seafloor due to the large angle of incidence caused by the low-altitude survey.

2.3. Map Generator

The task of the map generator is to update a map of the potential seafloor ahead of the vehicle based on the raw measurements of the scanning sonar, or the intensities of the sound waves reflected by seafloor. Measure-

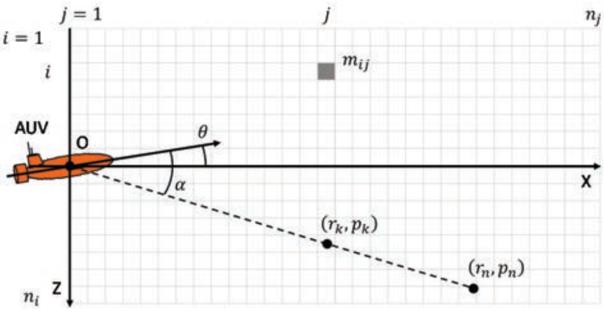

Fig. 3. Reflection intensity map. The map is a grid map whose origin is fixed to the AUV. Parameters used to construct the map are also indicated (see text for their definition).

ments of other perceptional sensors, if any, can also be utilized. The objective is to create a reflection intensity map defined as a grid map on the vertical plane along the vehicle's track (see **Fig. 3**). The origin of the map is fixed to the vehicle. Therefore, the map always covers a certain area in front of the vehicle, supposing the vehicle is horizontal (roll and pitch angles are zero). The value at the i-th row and the j-th column is defined as m_{ij}.

A measurement of a scanning sonar at time t is defined as follows:

$$S_t = \{\alpha, (r_1, p_1), (r_2, p_2), \dots, (r_n, p_n)\}, \quad \dots \quad (1)$$

where α represents the bearing angle of the acoustic beam, r and p represent the distance and reflection intensity, respectively, at each bin, and n is the number of bins. The map is recursively updated using the sonar measurement, S, the vehicle's pitch angle, θ, the surge velocity, u, and the depth, d. Firstly, all the values of the map are shifted by $(-dx, -dz)$ to represent the movement of the vehicle. The movement of the vehicle in the horizontal direction, dx, and the vertical direction, dz, are represented as follows:

$$dx = u_t \Delta t \tan\theta_t, \quad \dots \quad (2)$$

$$dz = d_t - d_{t-1}, \quad \dots \quad (3)$$

assuming the current time, t, and the update interval, Δt. Then, a Gaussian filter with the standard deviation of σ is applied to the map, to blur the values reflecting the ambiguity of the sensor measurements. The parameter σ should be defined on the basis of the reliability of the sensors and the ideal altitude of the vehicle. After that, the sonar measurement, S, is applied to the map. The application process for the k-th bin is described as follows:

$$m_{ij} = p_k(i, j \in R(\theta, \alpha, r_k)), \quad \dots \quad (4)$$

where R indicates the region covered by the k-th bin and i and j indicate the location of the cell, m_{ij}, in the z and x direction, respectively (see **Fig. 3**). R is a function of the vehicle's pitch angle (θ), the sonar's bearing angle (α), and the range (r_k), and it should be defined based on the spread of the acoustic beam. This process is performed for all the bins ($k = 1, \dots, n$).

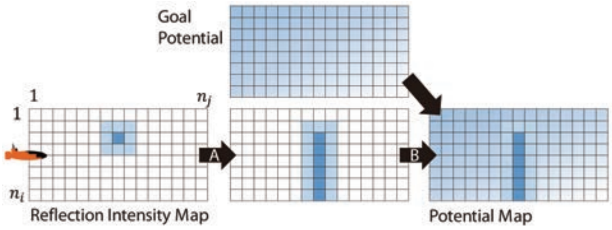

Fig. 4. Procedure to obtain the potential map.

2.4. Path Planner

The path planner estimates an ideal path for the AUV to follow the seafloor at a constant low altitude without collision, and then it generates a control reference value for the pitch angle. The proposed method utilizes the potential method, based on the potential map calculated from the reflection intensity map.

The procedure to obtain the potential map is shown in **Fig. 4**. The reflection intensity map is first modified so that the deeper area always has a higher value than the shallow area (A in **Fig. 4**). After this process, all the values of the map, m_{ij}, satisfy the following condition:

$$m_{ij} = \max_{k=1,\dots,i} m_{kj}. \quad \dots \quad (5)$$

The aim of this process is to avoid generating a path which goes under any detected obstacles. Such a path risks the vehicle being stuck in overhangs.

The next step is to create the potential map by adding the goal potential which is a uniform slope down to the deepest, farthermost point of the map relative to the position of the AUV (B in **Fig. 4**). The purpose of the goal potential is to guide the vehicle forward and downward.

The reference pitch angle, θ_{ref}, is generated by the following equation:

$$\theta_{\mathrm{ref}} = \mathop{\arg\min}_{\theta_{\min}<\theta<\theta_{\max}} \left(\sum_{i,j \in L_\theta} m_{ij} \right), \quad \dots \quad (6)$$

where L_θ indicates a segment of length l, starting from the AUV with the elevation angle θ. The possible range of the pitch angle, from $\theta_{\min}$ to $\theta_{\max}$, is defined based on the actual pitch angle and kinetic performance of the vehicle.

3. HATTORI

HATTORI (Highly Agile Terrain Tracker for Ocean Research and Investigation) is a testbed autonomous underwater vehicle built in 2016 at the Institute of Industrial Science, The University of Tokyo. The vehicle is designed for rapid and efficient imaging of a rugged seafloor, such as the irregular surface of coral reefs. HATTORI is a lightweight, one-man portable vehicle that can be operated from any available boat.

Figure 5 and **Table 1** show the appearance and specifications of the vehicle, respectively. **Fig. 6** shows

Fig. 5. AUV HATTORI.

Table 1. Specifications of the HATTORI.

General	
Size	1.02 m (L) × 0.48 m (W) × 0.29 m (H)
Mass	18 kg
Max. speed	2.0 m/s
Max. depth	300 m
Thruster	Blue Robotics T200 × 4
Battery (Thruster)	Lipo 4S 16Ah × 1
Battery (Computer)	Lipo 3S 8Ah × 1
Communication	Wi-Fi, SeaTrac X010
Computer	Intel Compute Stick (Atom Z8300)
OS	Ubuntu 16.04 LTS
Software	ROS (Kinetic Kame)
Navigational Instruments	
Current	Kenek VOT2-400-20TS
Depth	Blue Robotics Bar30
Attitude & Heading	CJMCU 10DOF
Scanning Sonar	Tritech Micron
Position	GPS, SeaTrac X010
Imaging Instruments	
Camera	GoPro Hero 4 × 2
Light	15W LED × 2, Sheet laser × 1

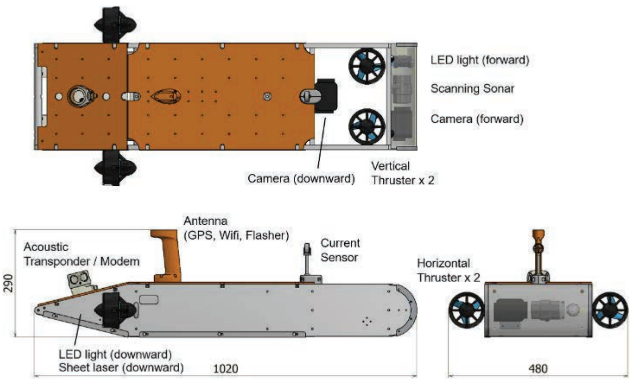

Fig. 6. General arrangement of the HATTORI (lengths are in mm).

schematic views of the vehicle highlighting the general design. The HATTORI is controlled by four thrusters: two horizontal thrusters for surge and yaw and two vertical thrusters for roll and pitch. The vertical thrusters are placed at the nose end to maximize pitch moment. The vehicle has a scanning sonar on its nose for seafloor detection. The scanning sonar has a beam frequency of 675 kHz, a maximum range of 100 m, and a beam width of $3 \times 30°$. Other on-board sensors include a magnetic compass, an attitude (roll and pitch) sensor, a depth sensor, and a water current sensor to measure surge velocity.

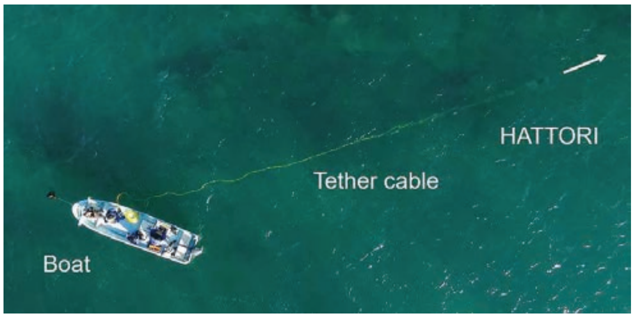

Fig. 7. The vehicle being deployed at Miura Peninsula.

The vehicle is equipped with two GoPro cameras paired with LED lights for illumination. One GoPro camera points downward and the other points forward. There is a sheet laser pointing downward which measures bathymetry by a light sectioning method [18]. The vehicle has a limited payload space around the vertical thrusters and on the top face.

The software was developed using the Robot Operating System (ROS) [a], which enables rapid development and easy adoption of new algorithms. The PID controllers were implemented for roll, pitch, heading, and surge velocity. A complementary filter [19] has been applied to reliably estimate the heading angle using a low-cost magnetic compass.

4. Sea Experiments

The proposed method was implemented in the HATTORI and a series of sea experiments was conducted to evaluate its performance. Results of two sea trials are presented in this paper. During both trials, the vehicle was deployed from a boat and was attached to a tether cable for easy retrieval and debugging. The update interval, Δt in Eq. (2), was set to be 0.2 s.

4.1. Rocky Shore

The first trials were carried out near Miura Peninsula, Japan, in December 2016. The terrain tracking test was performed over a rocky bottom at a depth of 1–5 m (**Fig. 7**). The reference surge velocity was 0.8 m/s. The settings of the scanning sonar were as follows: a maximum range of 20 m, a resolution of 0.05 m ($n = 400$), and a scan sector of $-45°$ to $45°$. The map parameters consist of a grid size of 0.05 m with the number of grids $(n_i, n_j) = (200, 400)$. Therefore, the actual coverage of the map is 10 m vertically and 20 m horizontally. The standard deviation of the Gaussian filter, σ, was set to be 1.5 (in grid units).

The vehicle succeeded in following 90 m of the rocky terrain in 130 s (**Fig. 8**). The travel distance was estimated by integrating current velocity measurements. The seafloor position was estimated based on scanning sonar measurements made when the beam direction was pointing downward ($> 30°$ from the horizontal) to maximize

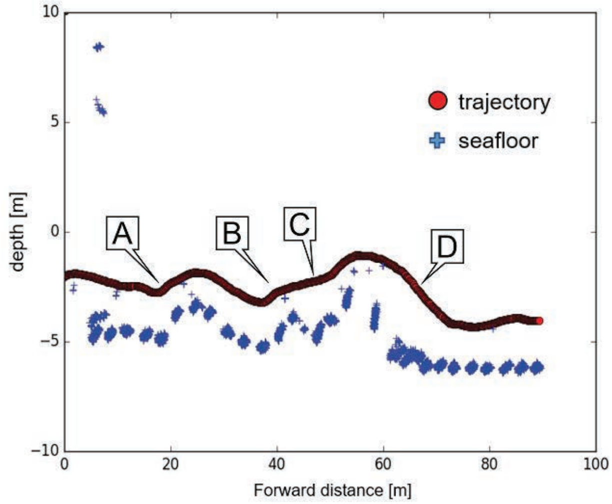

Fig. 8. The trajectory of the vehicle in the vertical plane (red line). The blue dots indicate the position of the seafloor estimated from scanning sonar measurements. The vertical axis is scaled by a factor of five compared to the horizontal axis.

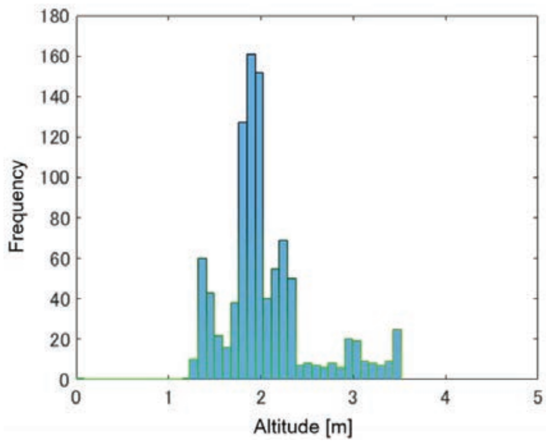

Fig. 9. A histogram of the altitude of the vehicle ($\sigma = 1.5$).

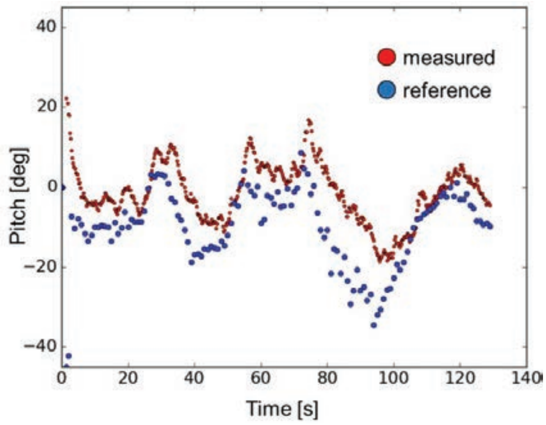

Fig. 10. The pitch angle of the vehicle, θ, and its control reference, θ_{ref}.

their reliability. The altitude was maintained between 1.5 and 2.5 m for most of the duration of the experiment, as indicated by the histogram of the altitude of the vehicle (**Fig. 9**). **Fig. 10** shows the time series of the pitch angle and its reference. There is a good correspondence between them, with a steady-state error of approximately 5° (see 10–20, 45, 60–65, and 120 s). The cause of the steady-state error is considered to be the righting moment of the vehicle.

Comparing the potential maps and the suggested paths obtained in real-time with the seafloor position, clearly indicates that the vehicle successfully detected obstacles along its path. **Figs. 11–14** show the potential maps when the vehicle was at the points A, B, C, and D in **Fig. 8**, respectively. Each cell of the potential map is colored depending on its value, m_{ij}. The value in increasing order is blue, green, yellow, and red. Rock mounds ahead of the vehicle shown in **Fig. 8** also appear very distinctly in the potential maps. Specifically, the largest mound encountered (about 12 m ahead of point B) is recognized on the potential map in **Fig. 12**. After crossing the mound (point D), the reference path curves down again to follow the relatively flat terrain stretching beyond the mound at lower elevations, as shown in **Figs. 13** and **14**. In addition, a 3D image of the seafloor obtained from the downward looking camera can easily be created using commercial software [b] (**Fig. 15**).

The same trial was performed again with a different value of sigma ($\sigma = 2.0$) in order to evaluate the capability of controlling the reference altitude. During this trial, the average altitude was raised from 1.9 m to 2.3 m (**Fig. 16**). Therefore, we conclude that the reference altitude can be controlled by adjusting σ. However, it is difficult to expressly define the reference altitude by σ, as the actual tracking altitude depends not only on σ but also on every parameter that affects the sonar measurements, such as the type of bottom sediment, the shape of the seafloor, and the physical relationship between the vehicle and seafloor.

4.2. Coral Reefs

In May 2017, the vehicle was deployed to evaluate the feasibility of this method to survey coral reefs. The location was Sekisei Lagoon, situated just west of Ishigaki Island, Okinawa. This area is known to be a hotspot of marine biodiversity in the Ryukyu Islands [20]. During the four-day survey period, the vehicle was deployed more than 50 times at several locations, from shallow (e.g., Taketomi Onsen, depth 20 m) to deep settings (Kataguwa, depth 60 m).

In this paper, we present the results of a trial conducted at Taketomi-kita (24.3541°N, 124.0783°E). The depth of this site is around 40 m. Throughout the dive, the vehicle was set to maintain a uniform direction with a heading reference of −90° (west) and a constant surge velocity of 0.5 m/s. The pitch angle was controlled by the tracking method described herein to follow the seafloor at a constant altitude. The parameter σ was set to 2.0 in order to maintain an altitude of approximately 2.3 m.

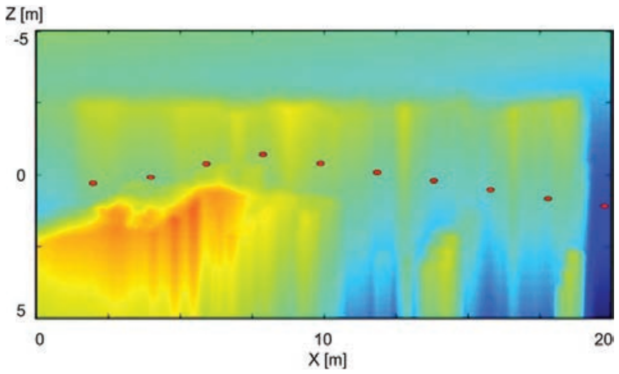

Fig. 11. Potential map and suggested path at point A in **Fig. 8**.

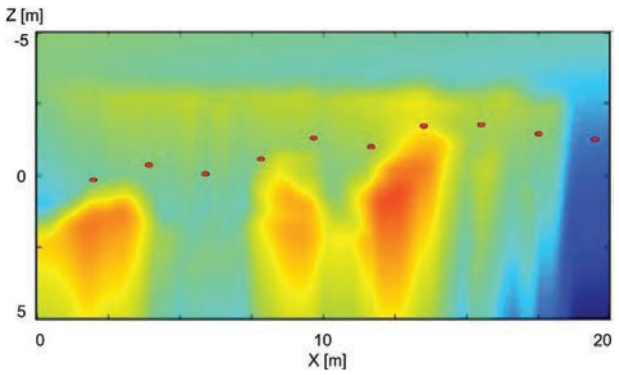

Fig. 12. Potential map and suggested path at point B in **Fig. 8**.

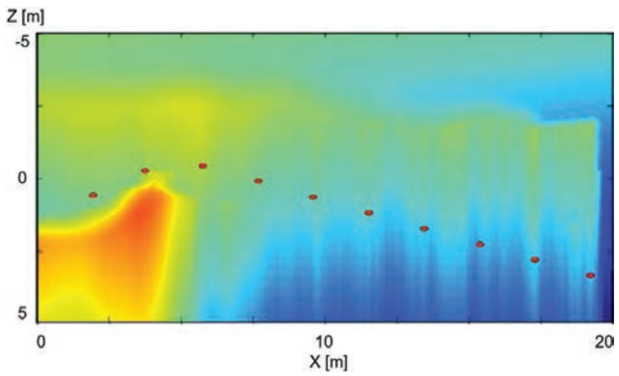

Fig. 13. Potential map and suggested path at point C in **Fig. 8**.

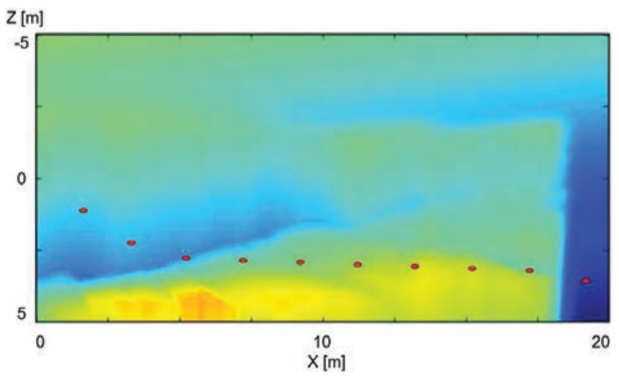

Fig. 14. Potential map and suggested path at point D in **Fig. 8**.

Fig. 15. A 3D image of the seafloor obtained from the downward looking camera and commercial software. The length is about 10 m.

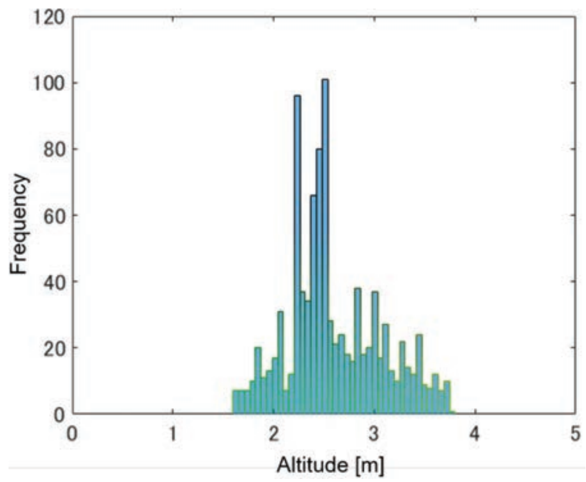

Fig. 16. A histogram of the altitude of the vehicle ($\sigma = 2.0$).

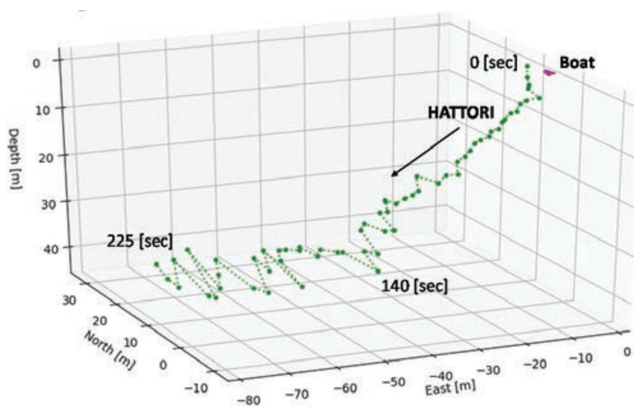

Fig. 17. The trajectory of the vehicle measured by the boat mounted USBL.

Figure 17 shows the trajectory of the vehicle acoustically measured from the boat using an Ultra Short Base Line device (USBL, model SeaTrac X150). The vehicle reached the seafloor in about 140 s, and then tracked the seafloor for about 40 m in 85 s. The zigzag motions seen after 140 s were estimated to be caused by USBL noise, considering the measurements of the onboard sensors shown in **Fig. 18**. The deviation of the yaw angle was within 6° from the reference of $-90°$ after 140 s, when the vehicle reached the seafloor. The mission was manually aborted because the entire length of the tether cable was used.

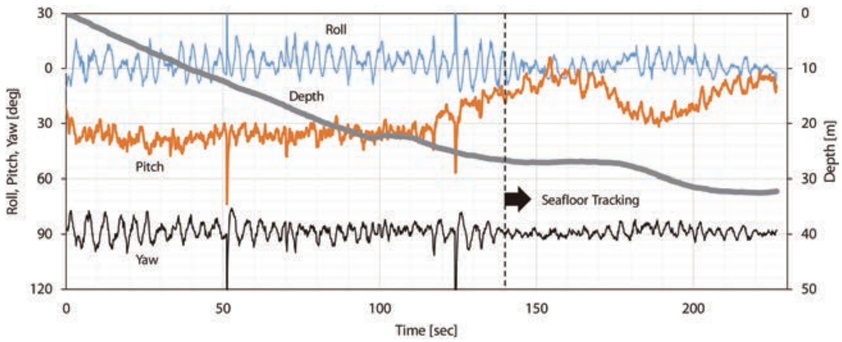

Fig. 18. Attitude and depth of the vehicle during the dive, measured by onboard sensors. The time definition is the same as **Fig. 17**. The spikes at 51 and 124 s are from noise.

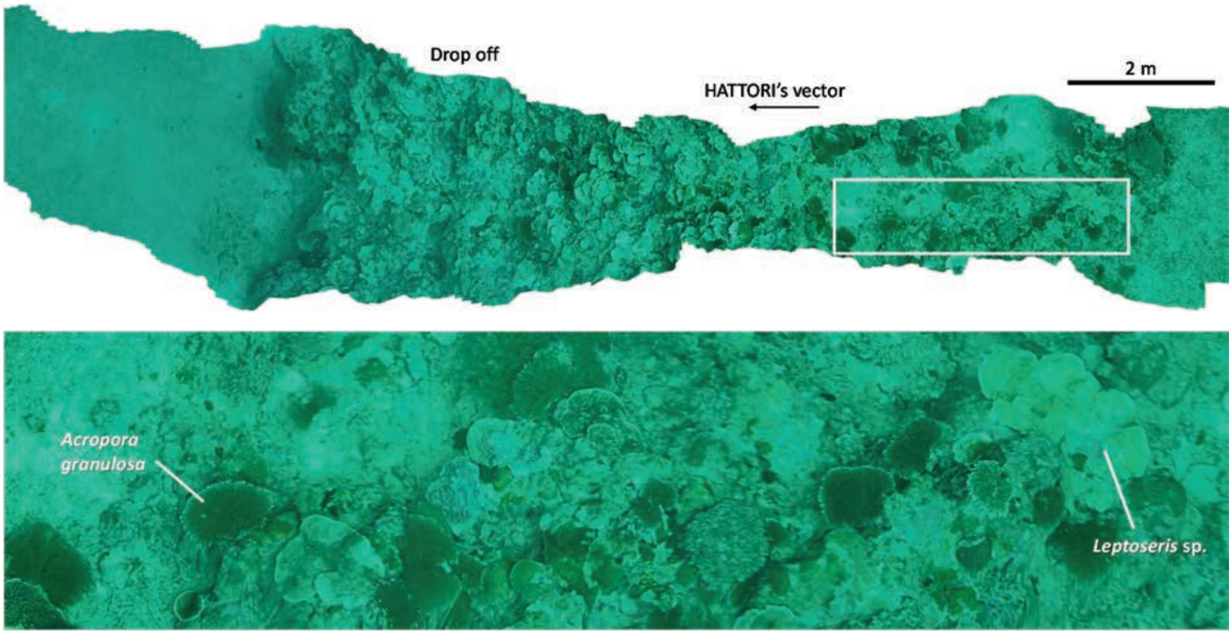

Fig. 19. Top: a photomosaic of the seafloor created from a video taken by the vehicle while tracking the seafloor. The photomosaic is orthorectified. The scale bar is shown at the top right. The vehicle traveled from right to left. Bottom: an enlarged view of the section indicated by the white rectangle. The size is 4×1 m.

A dense coral community composed of diverse species can be seen very clearly on a photomosaic of the seafloor created with the software mentioned previously and based on video images taken by the downward looking camera (**Fig. 19**). A steep drop-off is also visible in the middle left of the photomosaic. The height of the drop off is more than 5 m, according to the depth of the vehicle shown in **Fig. 18**. A sandy bottom lies to the left of the drop off. The resolution of the photomosaic is generally high enough for taxonomic identification of corals. Some areas of the photomosaic, however, are blurred due to the roll and pitch instability of the vehicle. As the vehicle was tethered, external forces related to waves and currents influenced its stability. Removing the tether cable will improve the stability of the vehicle and quality of the photomosaic.

5. Conclusion

For cruising-type AUVs operating on a rugged seafloor, solving the problem of obstacle avoidance is crucial. In this paper, we have demonstrated the reliability of a new terrain tracking method that works without high-grade sensors, such as INS, DVL, or multi-beam sonar, and can be implemented in lightweight AUVs. This method estimates seafloor position based on a reflection intensity map defined on a vertical plane and created using measurements taken by a scanning sonar and basic sensors of depth, attitude, and surge velocity. A reference pitch angle is generated to follow the seafloor at a constant altitude based on the potential method.

Sea experiments carried out with the AUV HATTORI, a lightweight, low-cost testbed designed for rapid and efficient imaging of a rugged seafloor, such as coral reefs, demonstrated the validity of the proposed method. During sea trials at Miura Peninsula, the vehicle succeeded in following a rocky terrain while maintaining an altitude of approximately 2 m and a surge velocity of approximately 0.8 m/s. Sea trials were conducted in and around the Sekisei Lagoon, a large lagoon enclosed by coral reefs; these trials demonstrated the potential usefulness of the method for rapid and effective visual assessment of the biotic and sedimentary components of the seafloor and local topography based on photomosaic images.

Acknowledgements

The authors are very grateful to Mr. Yarabu, Mr. Uehara, and Mr. Suzuki for their support in the experiments conducted at the Sekisei Lagoon. The authors also would like to thank to Mr. Kohtsuka and the staff of Misaki Marine Biological Station at The University of Tokyo for their help during the shallow sea trials at Miura Peninsula. This study was supported by JSPS KAKENHI Grant Number 16K17819 (M.H.) and 17H06218 (T.M.).

References:

[1] B. Bingham et al., "Robotic Tools for Deep Water Archaeology: Surveying an Ancient Shipwreck with an Autonomous Underwater Vehicle," J. of Field Robotics, Vol.27, No.6, pp. 702-717, 2010.

[2] T. Maki, A. Kume and T. Ura, "Volumetric mapping of tubeworm colonies in Kagoshima Bay through autonomous robotic surveys," Deep Sea Research Part I: Oceanographic Research Papers, Vol.58, No.7, pp. 757-767, 2011.

[3] Y. Nishida et al., "Autonomous Underwater Vehicle "BOSS-A" for Acoustic and Visual Survey of Manganese Crusts," J. Robot. Mechatron., Vol.28, No.1, pp. 91-94, 2016.

[4] S. B. Williams et al., "Monitoring of Benthic Reference Sites Using an Autonomous Underwater Vehicle," IEEE Robotics & Automation Magazine, Vol.19, No.1, pp. 73-84, 2012.

[5] M. Johnson-Roberson et al., "High-Resolution Underwater Robotic Vision-Based Mapping and Three-Dimensional Reconstruction for Archaeology," J. of Field Robotics, Vol.34, No.4, pp. 625-643, 2017.

[6] Y. Nishida et al., "Underwater Platform for Intelligent Robotics and its Application in Two Visual Tracking Systems," J. Robot. Mechatron., Vol.30, No.2, pp. 238-247, 2018.

[7] T. Maki et al., "AUV Tri-TON 2: An intelligent platform for detailed survey of hydrothermal vent fields," 2014 IEEE/OES Autonomous Underwater Vehicles (AUV), 2014.

[8] V. H. Fernandes, A. A. Neto, and D. D. Rodrigues, "Pipeline inspection with AUV," 2015 IEEE/OES Acoustics in Underwater Geosciences Symp. (RIO Acoustics), 2015.

[9] Y. Nishida et al., "Autonomous Underwater Vehicle "Tuna-Sand" for Image Observation of the Seafloor at a Low Altitude," J. Robot. Mechatron., Vol.26, No.4, pp. 519-521, 2014.

[10] T. Maki et al., "Low altitude tracking of rugged seafloors for autonomous visual observation," 2007 Symp. on, Underwater Technology and Workshop on Scientific Use of Submarine Cables and Related Technologies, pp. 488-494, 2007.

[11] T. Maki et al., "AUV HATTORI: a Lightweight Platform for High-speed Low-altitude Survey of Rough Terrains," OCEANS 2017 MTS/IEEE Anchorage, 2017.

[12] S. McPhail, M. Furlong, and M. Pebody, "Low-altitude terrain following and collision avoidance in a flight-class autonomous underwater vehicle," Proc. of the Institution of Mechanical Engineers Part M: J. of Engineering for the Maritime Environment, Vol.224, No.4, pp. 279-292, 2010.

[13] K. J. Morris et al., "A new method for ecological surveying of the abyss using autonomous underwater vehicle photography," Limnology and Oceanography-Methods, Vol.12, No.11, pp. 795-809, 2014.

[14] S. M. Schillai et al., "Evaluation of Terrain Collision Risks for Flight Style Autonomous Underwater Vehicles," 2016 IEEE/OES Autonomous Underwater Vehicles (AUV), pp. 311-318, 2016.

[15] Y. Noguchi, Y. Kuranaga, and T. Maki, "Adaptive navigation of a high speed autonomous underwater vehicle using low cost sensors for low-altitude survey," 2017 IEEE Underwater Technology (UT), 2017.

[16] F.-G. Ding et al., "AUV local path planning based on virtual potential field," 2005 IEEE Int. Conf. Mechatronics and Automations, Vol.4, pp. 1711-1716, 2005.

[17] V. Ganesan, M. Chitre, and E. Brekke, "Robust underwater obstacle detection and collision avoidance," Autonomous Robots, Vol.40, No.7, pp. 1165-1185, 2016.

[18] H. Kondo et al. "Relative navigation of an autonomous underwater vehicle using a light-section profiling system," 2004 IEEE/RSJ Int. Conf. on Intelligent Robots and Systems (IROS), Vol.2, pp. 1096-1102, 2004.

[19] M. Euston et al., "A Complementary Filter for Attitude Estimation of a Fixed-Wing UAV," 2008 IEEE/RSJ Int. Conf. on Intelligent Robots and Systems (IROS), Vol.1-3, pp. 340-345, 2008.

[20] The Ministry of the Environment, "Coral Reefs of Japan," The Ministry of the Environment, 2004.

Supporting Online Materials:

[a] The Robot Operatin System (ROS), http://www.ros.org [Accessed June 24, 2017]

[b] Agisoft PhotoScan, http://www.agisoft.com [Accessed June 25, 2017]

Name:
Toshihiro Maki

Affiliation:
Associate Professor, Institute of Industrial Science, The University of Tokyo

Address:
4-6-1 Komaba, Meguro-ku, Tokyo 153-8505, Japan

Brief Biographical History:

2008- Research Associate, The University of Tokyo
2010- Associate Professor, The University of Tokyo
2015 Guest Investigator, Woods Hole Oceanographic Institution

Main Works:

• "Volumetric mapping of tubeworm colonies in Kagoshima Bay through autonomous robotic surveys," Deep Sea Research Part I: Oceanographic Research Papers, Vol.58, No.7, pp. 757-767, 2011.

Membership in Academic Societies:

• The Institute of Electrical and Electronics Engineers (IEEE) Oceanic Engineering Society (OES)
• The Japan Society of Naval Architects and Ocean Engineers (JASNAOE)
• The Japan Society for Marine Surveys and Technology
• Marine Acoustics Society of Japan (MASJ)
• The Robotics Society Japan (RSJ)

Name:
Yukiyasu Noguchi

Affiliation:
Graduate Student, Institute of Industrial Science, The University of Tokyo

Address:
4-6-1 Komaba, Meguro-ku, Tokyo 153-8505, Japan

Brief Biographical History:

2016- Master Course Student, The University of Tokyo
2018- Doctor Course Student, The University of Tokyo

Main Works:

• "Adaptive navigation of a high speed autonomous underwater vehicle using low cost sensors for low-altitude survey," 2017 IEEE Underwater Technology (UT), pp. 1-4, 2017.

Membership in Academic Societies:

• IEEE Oceanic Engineering Society (OES)
• The Robotics Society Japan (RSJ)
• The Japan Society of Mechanical Engineers (JSME)

Name:
Yoshinori Kuranaga

Affiliation:
Graduate Student, Institute of Industrial Science, The University of Tokyo
Nomura Research Institute, Ltd. (Current)

Address:
4-6-1 Komaba Meguro-ku, Tokyo 153-8505, Japan

Brief Biographical History:
2015- Master Course Student, The University of Tokyo
2017- Joined Nomura Research Institute, Ltd.

Name:
Kotohiro Masuda

Affiliation:
Project Researcher, Center for Integrated Underwater Observation Technology, Institute of Industrial Science, The University of Tokyo

Address:
4-6-1 Komaba, Meguro-ku, Tokyo 153-8505, Japan

Brief Biographical History:
2011- Joined Bellnix Co., Ltd. (2013 Resign)
2013- Trainees in Maki Lab, Institute of Industrial Science, The University of Tokyo
2015- Project Research Specialist in Maki Lab, Institute of Industrial Science, The University of Tokyo
2016- Project Researcher in Maki Lab, Center for Integrated Underwater Observation Technology, Institute of Industrial Science, The University of Tokyo

Main Works:
• "Docking Method for a Hovering-Type AUVs Based on Acoustic and Optical Landmarks," J. Robot. Mechatron., Vol.30, No.1, pp. 55-64, 2018.

Membership in Academic Societies:
• The Robotics Society of Japan (RSJ)

Name:
Takashi Sakamaki

Affiliation:
Senior Technical Specialist, Institute of Industrial Science, The University of Tokyo

Address:
4-6-1 Komaba, Meguro-ku, Tokyo 153-8505, Japan

Brief Biographical History:
1980 Institute of Industrial Science, The University of Tokyo

Main Works:
• "Docking Method for a Hovering-Type AUVs Based on Acoustic and Optical Landmarks," J. Robot. Mechatron., Vol.30, No.1, pp. 55-64, 2018.

Membership in Academic Societies:
• The Japan Society of Mechanical Engineers (JSME)

Name:
Marc Humblet

Affiliation:
Associate Professor, Department of Earth and Planetary Sciences, Nagoya University

Address:
Furo-cho, Chikusa-ku, Nagoya 464-8601, Japan

Brief Biographical History:
2008- Postdoctoral Fellow, The University of Tokyo
2011- Associate Professor, Nagoya University

Main Works:
• "Coral community changes in the Great Barrier Reef in response to major environmental changes over glacial-interglacial timescales," Palaeogeography, Palaeoclimatology, Palaeoecology, Vol.472, pp. 216-235, 2017.

Membership in Academic Societies:
• The International Society for Reef Studies (ISRS)
• The Japanese Coral Reef Society (JCRS)
• The Geological Society of Japan (GSJ)
• The Japan Geoscience Union (JGU)

Name:
Yasuo Furushima

Affiliation:
Deputy Group Leader (Senior Engineer), Research and Development (R&D) Center for Submarine Resources, Environmental Impact Assessment Research Group, Japan Agency for Marine-Earth Science and Technology (JAMSTEC)

Address:
2-15 Natsushima-cho, Yokosuka 237-0061, Japan

Brief Biographical History:
1997- Research Scientist, Japan Agency for Marine-Earth Science and Technology (JAMSTEC)
2014- Senior Engineer, JAMSTEC
2018- Deputy Group Leader, JAMSTEC

Main Works:
• "Periodic Behavior of Abyssal Flow in Okinawa Trough Hydrothermal Fields," Proc. of the 28th Int. Ocean and Polar Engineering Conf. Sapporo (ISOPE), pp. 119-123, 2018.

Membership in Academic Societies:
• Marine Technology Society (MTS)
• International Society for Reef Studies (ISRS)
• The Japanese Society of Fisheries Oceanography (JSFO)
• The Oceanographic Society of Japan (JOS)
• Japanese Association for Coastal Zone Studies (JACZS)
• The Japanese Coral Reef Society (JCRS)